

ELECTRIC RESPONSE OF HIGH LATITUDINAL MIDDLE ATMOSPHERE TO SOLAR WIND CHARACTERISTICS STUDIED BY MODEL SIMULATIONS

Peter Tonev

Space Research and Technology Institute – Bulgarian Academy of Sciences
e-mail: ptonev@bas.bg

Keywords: ionospheric potential, DC global atmospheric electrical circuit, ionospheric conductivity, atmospheric conductivity, field-aligned currents, Weimer model, ionosphere-ground current, continuity equation

Abstract: The role of the non-uniform distribution of the ionospheric potential V_I in each hemisphere at polar latitudes (characterized by trans-polar potential difference V_{IP} of 30-140 kV) is studied in the global atmospheric electrical circuit (AEC) below 100 km. The potential difference V_{IP} is controlled by the solar wind (SW) parameters, hence, our goal is to estimate the AEC response to solar wind and solar activity. A numerical model is developed which serves to determine the electric currents and fields thus superimposed to basic 'fair-weather' AEC characteristics. This model is based on the continuity equation for the electric current density. Computations are made in the domain of altitudes 50-160 km at geomagnetic latitudes higher than 45° of a hemisphere. Sources for the superimposed electric currents and fields are the trans-polar potential difference V_{IP} and the field-aligned currents at altitude 160 km. This upper boundary of the model domain is above the dynamo-region in which an effective closure of field-aligned currents is realized. We compare the superimposed currents and fields to AEC characteristics in lower ionosphere and mesosphere and show that these first are dominating in these regions. The influence of the IMF and SW variations on the dominating superposed electric currents and fields is studied. Their possible effects on the atmospheric parameters and processes are considered.

ЕЛЕКТРИЧЕСКА РЕАКЦИЯ НА ВИСОКОШИРОТНАТА СРЕДНА АТМОСФЕРА НА ХАРАКТЕРИСТИКИТЕ НА СЛЪНЧЕВИЯ ВЯТЪР, ПОЛУЧЕНА ЧРЕЗ СИМУЛАЦИОНЕН МОДЕЛ

Петър Тонев

Институт за космически изследвания и технологии - Българска академия на науките
e-mail: ptonev@bas.bg

Ключови думи: йоносферен потенциал, DC глобална атмосферна електрическа верига, йоносферна проводимост, атмосферна проводимост, надлъжни токове, модел на Weimer, ток йоносфера-земя, уравнение на непрекъснатостта

Резюме: Изследва се ролята на нееднородното разпределение на йоносферния потенциал V_I на високи ширини (той се характеризира с транс-полярна потенциална разлика $V_{IP} = 30-140$ kV) в глобалната атмосферна електрическа верига (АЕВ) под 100 km. Транс-полярната потенциална разлика V_{IP} се управлява от параметрите на слънчевия вятър, следователно, целта ни е да се направи оценка на реакцията на АЕВ на слънчевия вятър и слънчевата активност. Развита е числен модел, чрез който да се определят електрическите токове и полета добавени към основните величини 'при ясно време' в АЕВ. Този модел е базиран върху уравнението за непрекъснатост на плътността на електрическия ток. Направените изчисления са за височинната област 50-160 km на геомагнитни ширини над 45° в дадена полусфера. Като източници на въпросните добавени електрически токове и полета се приемат потенциалната разлика на транс-полярния потенциал V_{IP} и надлъжните токове на височина 160 km. Тази горна граница на моделната област е над динамо-областта, в която се осъществява ефективно затваряне на надлъжните токове. Направено е сравнение на добавените електрически токове и полета със съответните базови в АЕВ и е показано, че първите доминират в тези области. Изследвано е влиянието на вариациите на междупланетното магнитно поле и на слънчевия вятър върху тези доминиращи електрически токове и полета. Разгледани са възможните им ефекти върху атмосферните параметри и процеси.

Introduction

According to the classical view, the DC global atmospheric electric circuit (AEC) [1,2] is determined by the electric currents generated by distributed over the globe lightning-producing thunderstorms (TS), and electrified shower clouds (ESC) producing currents only by dissipation of their electric charges [2,3]. According to recent observations [1-3], the global rate of the lightning discharges is about 50 s^{-1} .

The upward currents from TSs and ESCs charge the ionosphere to a positive potential V_i of 250-300 kV with respect to ground; their closure is by the fair-weather downward current of density $1\text{-}6 \text{ pA}\cdot\text{m}^{-2}$ [1-3] flowing from the ionosphere to the surface. An additional source takes place at high latitudes [4], and its contribution to AEC is estimated here: it is related to interaction of solar wind (SW) with magnetosphere and ionosphere, and is realized by the system of field-aligned currents (FAC) and the formation of trans-polar potential difference V_{TP} of 30-140 kV in each hemisphere superimposed to the uniformly distributed ionospheric potential V_i . The influence of the potential difference V_{TP} on AEC is examined here; this needs consideration of both sources.

At any moment in AEC operate about 1000 thunderstorms, most of them located at equatorial and low latitudes [3]: they produce cloud-ground lightning discharges realizing a temporal shortcut in the cloud-ground link in AEC [5] (unlike intracloud discharges). This link forms a bottleneck in AEC because of its large resistance [5, 6] in respect to the other AEC links; hence the contribution in AEC of lightning may be significant (its contribution is estimated between 2% [6] and 40% or more [5]). The ESCs contribute to the ionosphere by currents from dissipating cloud charges.

The electric currents in AEC exist due to ionization of the atmosphere (although weak), which provides conductivity. Different sources of ionization play a role in atmospheric regions. Between 3 km and 70-80 km galactic cosmic rays (GCR) contribute for ionization [7-9], so that up to 35 km GCR are the only ionization source [10-12]. Below 3 km the radioactive gases (radon, etc.) of terrestrial origin [13] are the only ionization source (photo-ionization plays a role above 35 km). In the high latitudinal ionosphere there are different additional ionization sources, e.g. precipitation particles, intense electric currents in auroral regions, GCR [8, 9], solar cosmic rays [14], anomalous cosmic rays [15], etc. These factors play an important role in formation of the ionospheric conductivity at high latitudes which has a key role in formation and distributions of the electric currents and fields in AEC originating from the potential difference V_{TP} and superimposed to those originating by TSs and ESCs. The ionospheric electron density can also be influenced by electric fields generated above powerful thunderstorms [16].

Our goal is to evaluate by means of modeling the superimposed electric currents and fields at high latitudes generated by the SW-magnetosphere-ionosphere interactions considered above, and their relative role in AEC [17]. If such superimposed electric currents exist, they can form a very small 'residual' part of FAC due to their incomplete closure in the dynamo region. The closure of these 'residual' currents occurs mainly in the lower ionosphere, below 100 km, so that they will diminish quickly with lowering of the altitude. That is why we estimate the superimposed electric currents and related fields first in the lower ionosphere and mesosphere. For this goal, a 3D numerical model is developed, based on the continuity equation for the electric current density. Computations are made in the domain of altitudes 50-160 km at geomagnetic latitudes higher than 45° of one (north or south) of the hemispheres. The sources of the currents and fields studied (the trans-polar potential difference V_{TP} and FAC at altitude 160 km) are taken in account as model boundary conditions.

Several facts support the idea that significant electric currents and fields can penetrate from the ionosphere dynamo-region to downward: *i)* The horizontal scale of the region of FAC and trans-polar potential is ~ 3000 km (or more during disturbed geomagnetic conditions) – tens of times larger than the vertical dimension of the region of interest [4]; *ii)* The magnitude of the potential difference V_{TP} is comparable to the undisturbed ionospheric potential V_i . Different experimental and theoretical investigations support the possibility of penetration of 'residual' currents down to the Earth's surface. Experimental measurements [4,18] of the potential gradient and of air-earth current in Antarctica demonstrate that they correlate with the geomagnetic activity, actually due to the penetration of SW-controlled superimposed currents down to the ground. There are a series of theoretical investigations [19,20], which show a presence of significant superimposed electric fields in the high-latitudinal middle and lower atmosphere, and that these fields are re-oriented from horizontal in the middle atmosphere to vertical ones at the Earth's surface.

The estimations of the electric currents and fields superimposed to AEC, thus discussed, are useful in considerations of AEC as a possible link for the transmission of the solar influences to climate [21], and in revealing complex and incompletely understood system of links between: (a) AEC, conductivity and aerosols, the cloud microphysics which govern TS and ESC characteristics, global temperature, water content, climate, minor constituents [22,10] on one hand; (b) solar activity, galactic, solar and anomalous cosmic rays and high energy particles, on the other hand [9,11,12,15].

Simulation Model

A physically based numerical 3D steady-state model is proposed to determine the distributions of the electric current \mathbf{j} and related field \mathbf{E} in the region 0-100 km created by the electric potential V_P at altitude $Z_B=160$ km at polar geomagnetic (gm) latitudes, and superimposed to the respective characteristics of AEC. This altitude is above the dynamo-region in which an effective closure of FAC is realized. The continuity equation for \mathbf{j} is solved:

$$(1) \quad \nabla \cdot \mathbf{j} = 0, \quad \text{where} \quad \mathbf{j} = [\sigma]\mathbf{E}, \quad \mathbf{E} = -\nabla\Phi$$

In Eq.(1) Φ is the potential of \mathbf{E} , $\Phi(z=160 \text{ km}) = V_{TP}$, $[\sigma]$ represents the conductivity. Eq.(1) is solved in spherical coordinates in a domain bounded by altitudes 0-160 km and gm co-latitudes $\theta \leq 45^\circ$. The distributions of FAC and V_{TP} at altitude 160 km are determined for the specified SW parameters from the model of Weimer [23], and V_P is used as a boundary condition to Eq.(1). Eq.(1) is solved numerically in succeeding steps for separate thin (≤ 0.5 km) height layers at 3D grid consisted of 3D rectangular elements. A modification of finite volume method [24] is used by parameters controlled by the ratio between the field-aligned and vertical j_z , and the transverse and horizontal j_{PH} components of the superimposed current \mathbf{j} .

The modifications of the electric characteristics of AEC are evaluated as function of the SW parameters. First, the distribution of the vertical superimposed electric current j_z at altitudes below 100 km is studied by a representative set of variations of SW parameters and conditions of conductivity formation, and is compared (in different atmospheric regions, and at the surface) to the fair-weather current j_{FW} provided by tropospheric electrical sources. The sensitivity of j_z to variations of the key parameters for the geomagnetic activity (IMF components B_z , B_y , and of the solar wind velocity V_{SW}) are estimated. Computational results for the electric current j_z and field E_z are obtained in the mesosphere and lower ionosphere with respect of the specific conductivity status.

Input Data

Two types of input data are used in the model: *D1*) Data representing the response of the ionosphere to the SW-magnetosphere-ionosphere interaction close above the dynamo-region (related to FAC and superimposed electric potential at altitude of 160 km); *D2*) Conductivity in the model domain 0 - 160 km at latitudes $> 45^\circ$. The model of Weimer [23] is used to obtain the input data of type *D1* for specified steady-state parameters of the IMF and SW: B_y , B_z IMF components, the density N and velocity V_x of the SW plasma, the tilt of the Earth' axis related to SW plasma flow. Input data *D1* are presented by the 2D distributions of FAC and of the electric potential V_{TP} obtained from the Weimer model. Physically adequate data can also be obtained with the use of the SuperDARN radar network [25].

Input data of type *D2* are the spatial distributions of ionospheric conductivity (in region 80-160 km), and of atmospheric conductivity (between 0 and 80 km) in the model domain. The ionospheric conductivity is anisotropic and described by a tensor $[\sigma]$ characterized by three components: the field-aligned σ_0 , Pedersen σ_P , and Hall σ_H conductivities. It also depends on the inclination angle of the geomagnetic field lines. Here it is determined from equation $r/\sin^2\theta = const$ where r is the distance from the Earth's center, and θ is the geomagnetic (gm) co-latitude. The interactive Ionospheric Conductivity Model IRI2007 (<http://swdcwww.kugi.kyoto-u.ac.jp/ionocond/sigcal/index.html>) is used to represent 3D distributions of σ_0 , σ_P , and σ_H for a specified date, with account of space weather conditions. For polar latitudes data *D2* require to take into account different factors with a significant impact on conductivity [11] which add their contribution to formation of conductivity. In the atmospheric region 0-70 km we use a fixed 3D conductivity distribution of the scalar conductivity for moderate solar activity and undisturbed conditions obtained according to recent knowledge [3,13], and by the use of models [8,26-28]. The representation used takes into account dependency of the conductivity profile by diurnal distributions and latitude. Variations of this fixed conductivity distribution can take place due to solar activity change (in stratosphere, by modulated GCR [8]), due to volcano eruptions (leading to dramatic reduction of stratospheric conductivity in polar region [3,13]), and to pollution which takes place close to surface [13].

Results and conclusions

Seven sample cases related to sets of different SW parameters are shown in Table 1. The maximum (positive and negative) values of the electric potential V_{TP} and FAC density are demonstrated for each case. These values are obtained from the Weimer model [23]. Table 1 illustrates parameters characterizing the input data to our model in each case.

Computations of the superimposed electric current and field in the lower ionosphere 60 - 100

Table 1. Maximum & minimum values at boundary $z = 160$ km of the electric potential Φ and respective field-aligned currents j in sample cases, obtained from Weimer model [23]

Case N	B_y , nT	B_z , nT	V_x , km.s ⁻¹	Φ_{\max} , kV	Φ_{\min} , kV	$\Delta\Phi$, kV	$j(\Phi_{\max})$, $\mu\text{A}/\text{m}^2$	$j(\Phi_{\min})$, $\mu\text{A}/\text{m}^2$
1	0	8	400	11.3	-10.5	21.8	0.29	-0.31
2	2	4	400	14.9	-14.5	29.4	0.42	-0.27
3	0	-0.5	300	17.8	-20.6	38.4	0.60	-0.30
4	2	-2	400	31.4	-37.6	69.0	0.63	-0.57
5	-5	-5	400	50.0	-58.0	108.0	0.78	-0.82
6	-7	-10	500	65.8	-73.9	139.7	0.90	-0.86
7	-8	-14	600	88.6	-97.0	185.6	0.94	-1.10

km are made by data for the ionospheric conductivity obtained from IRI2007 for 21 March 2005. Figs. 2 and 3 illustrate results, for the distributions of the field-aligned electric current and field, respectively (below 70 km their vertical components are considered, instead) which are realized by solar wind parameters $B_y = -4$ nT, $B_z = -7$ nT, $V_x = 400$ km/s, $N = 8 \text{ cm}^{-3}$ and by tilt angle of the Earth axis = 0° , in the region of interest 60-100 km at four locations corresponding to different magnetic local time: 00:00, 06:00, 12:00, and 18:00. Fig.2 shows that the 'residual' current from FAC in this region decrease exponentially with altitude, but slower at lower heights (their scale-height becomes larger by small altitude z) because of the decrease of the effectiveness of their closure. At the region considered these currents are significantly larger than those generated in GEC by tropospheric sources.

Fig.3 shows the related field-aligned (vertical below 70 km) electric fields. These electric fields increase at lower altitudes; they can reach tens of mV/m at the lower ionosphere boundary (65-70 km). This increase is a result of the fact that below a definite altitude the closure by transverse currents becomes ineffective since the transverse resistance is larger than the resistance down to the surface.

Fig.4 demonstrates the sensitivity of the vertical electric field E_z studied by us to each of the considered parameters B_y (dashed curves 1), B_z (solid curves 2) and V_x (solid curves 3) at two altitudes (80 km and 70 km). The largest relative variations of this electric current are produced by component B_z when $B_z < 0$.

The DC aspects of AEC are considered here, and the relative role in it of the FAC and transpolar potential is estimated. The obtained results show that the SW-magnetosphere-ionosphere interactions considered lead to generation of non-neglecting electric fields in the lower ionosphere at high gm latitudes. These fields are controlled by the SW parameters and space weather, and possibly can contribute to processes like electron heating in the mesosphere. The question arises whether in some cases and under specific conditions the electric field superimposed in the mesosphere can be large enough to explain strong V/m electric fields which have being systematically observed at high latitudes [29] and which show correlation with the geomagnetic activity.

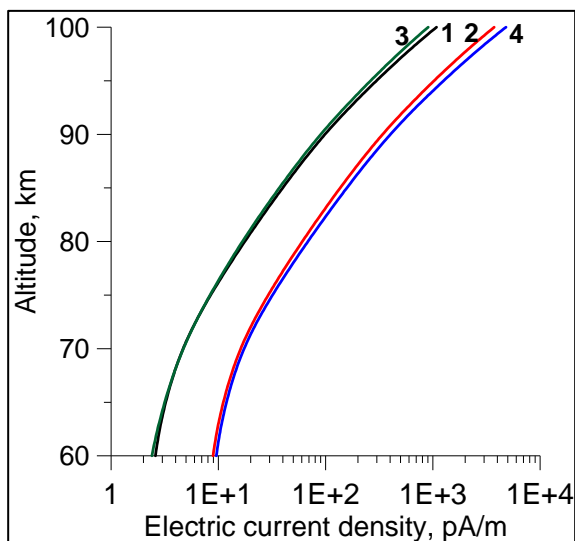


Fig. 1. Vertical superimposed electric current j_z as function of the altitude 60-100 km by gm longitudes at MLT = 00:00, 06:00, 12:00 and 18:00 (curves 1-4, respectively). The IMF - SW components: $B_y = 4$ nT, $B_z = 7$ nT, the tilt angle of the Earth is 0° , the plasma density is $N = 8 \text{ cm}^{-3}$, $V_x = 400$ km/s.

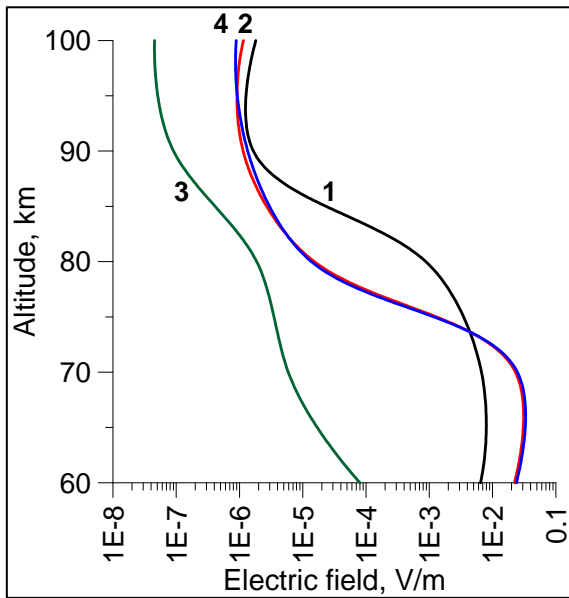


Fig. 2. Same as Fig.1, but for the vertical electric field E_z .

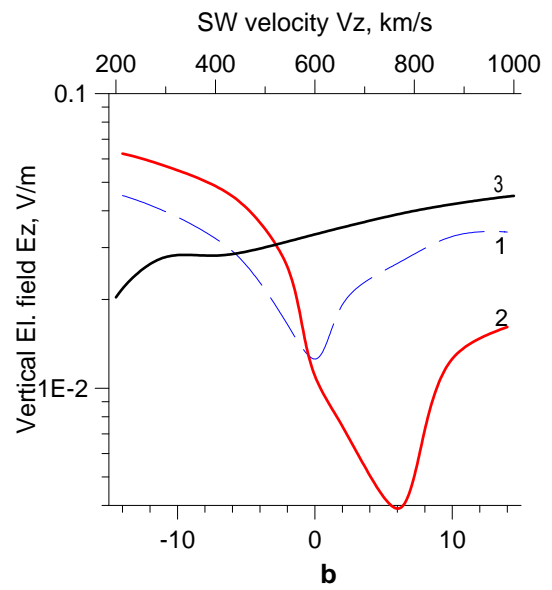
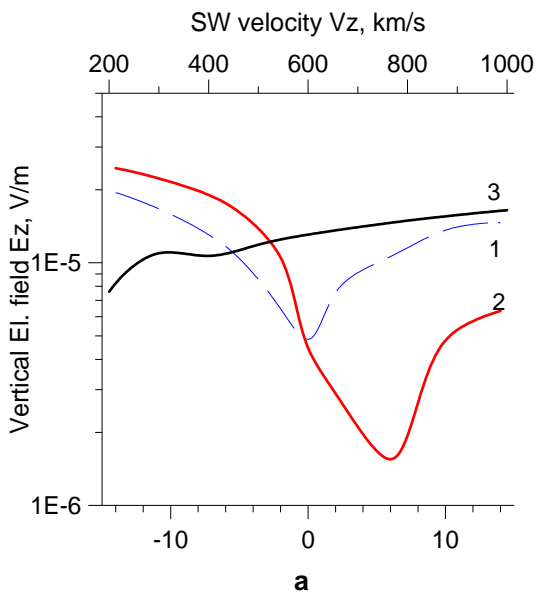


Fig. 4a, b. Maximum vertical superposed electric field E_z at altitudes 80 km (a) and 70 km (b) as function of the IMF components B_y (curve 1), B_z (2), and SW velocity V_z (3). B_y varies by fixed other parameters: $B_z=0$, tilt angle of the Earth 0° , plasma density $N = 8 \text{ cm}^{-3}$. $V_z = 600 \text{ km/s}$. B_z varies by $B_y=0$ and the same fixed parameters. Variations of the SW velocity V_z are by $V_z = 500 \text{ km/s}$, $B_y = 0$, $B_z = -3$, $N = 8 \text{ cm}^{-3}$.

References:

1. Bering, III, E.A., A.A.Few, J.R.Benbrook. The global electric circuit, *Physics Today*, 51 (10), 1998, 24-30.
2. Rycroft, M. J., S. Israelsson, C. Price. The global atmospheric electric circuit, solar activity and climate change, *J. Atmos. Sol-Terr. Phys.*, 62, (17-18), 2000, 1563-1576.
3. Rycroft, M.J., R.G. Harrison, et al. An overview of Earth's global electric circuit and atmospheric conductivity, *Space Sci Rev*, 137, 2008, 83-105, doi 10.1007/s11214-008-9368-6.
4. Tinsley, B.A. Influence of Solar Wind on the Global Electric Circuit and Inferred effects on Cloud Microphysics, Temperature and Dynamics in the Troposphere, *Space Sci. Rev.* 94 (1-2), 2000, 231-258.
5. Stozhkov, Y.I. The role of cosmic rays in the atmospheric processes, *J. Phys. G: Nucl. Part. Phys.* 29, 2003, 913-918.
6. Rycroft, M.J., A. Odzimek, et al., New model simulations of the global atmospheric electric circuit driven by thunderstorms and electrified shower clouds: The roles of lightning and sprites, *J. Atmos. Solar-Terr. Phys.*, 69, 2007, 2485-2509.
7. Usoskin, I., L. Desorgher, et al. Solar and Galactic Cosmic Rays in the Earth's Atmosphere. *Acta Geophysica*, 57, 2009, 1, 88-101.
8. Velinov, P.I.Y., L. Mateev. 1990, Effects of Galactic Cosmic Rays and High Energy Particles on the Parameters of the Global Atmospheric Electrical Circuit. *Geomagnetism and Aeronomy*, 30, 4, 554 - 557.
9. Velinov, P.I.Y., A. Mishev. 2007, Cosmic Ray Induced Ionization in the Atmosphere Estimated with CORSIKA Code Simulations. *C.R. Acad. bulg. Sci.*, 60, 5, 495-502.
10. Velinov, P.I.Y., 1968, On Enhanced Ionization in Lower Ionosphere of Polar Cap Due to Solar Corpuscular Fluxes. *Izvestia AN SSSR, phys.*, 32, 11, 1906-1909.
11. Velinov, P.I.Y., et al. 2001, Determination of Electron Production Rates Caused by Cosmic Ray Particles in Ionospheres of Terrestrial Planets. *J. Adv. Space Res.*, 27, 11, 1901-1908.
12. Velinov, P.I.Y., H. Ruder, et al. 2004, Method for Calculation of Ionization Profiles Caused by Cosmic Rays in Giant Planet Ionospheres from Jovian Group, *J. Adv. Space Res.*, 33, 2, 232-239.
13. Tinsley, B.A., L. Zhou. Initial results of a global circuit model with variable stratospheric and tropospheric aerosols, *J.Geoph.Res.*, 111, 2006, D16205.
14. Velinov, P.I.Y., 1970, Solar Cosmic Ray Ionization in the Low Ionosphere. *J. Atmos.Terr.Phys.*, 32, 139-147.
15. Velinov, P.I.Y., 1991, Effect of the Anomalous Cosmic Ray (ACR) Component on the High-Latitude Ionosphere. *Compt.rend. Acad. bulg. Sci.*, 44, 2, 33-36.
16. Velinov, P.I.Y., Chr. Spassov, S. Kolev. 1992, Ionospheric Effects of Lightning during the Increasing Part of Solar Cycle 22. *J. Atmosph. Terr. Phys.*, 54, 10, 1347-1353.
17. Tonev, P.T., Estimation of currents in global atmospheric electric circuit with account of transpolar ionospheric potential, *Compt.rend. Acad. bulg. Sci.*, 65, 5, 2012 (in press).
18. Corney, R.C., G.B. Burns, et al. The influence of polar-cap convection on the geoelectric field at Vostok, Antarctica, *J.Atmos. Solar-Terr. Phys*, 65, 2003, 345-354.
19. Park, C.G. Downward mapping of high-latitude ionospheric electric fields to the ground, *J. Geophys. Res.*, 81(1), 1976, 168-174.
20. Ptitsyna, N., T. J. Tuomi, et al. Magnetospheric-ionospheric effect on the ground-level atmospheric electric field at Helsinki, *J. Atmos. Sol-Ter. Phys.*, 59 (1), 1997, 99-105.
21. Harrison, R.G., The global atmospheric electrical circuit and climate Surveys in *Geophysics* 25, (5-6), 2004, 441-484, doi: 10.1007/s10712-004-5439-8.
22. Velinov, P.I.Y., N.A. Smirnova, V.A. Vlascov. Hybrid Quadri - Ionic Model of the Low Ionosphere. *J. Adv. Space Res.*, 4 (1), 123- 130, 1984.
23. Weimer, D.R. Models of high-latitude electric potentials derived with a least error fit of spherical harmonic coefficients, *J.Geoph.Res.*, 100, 1995, 19595-19608.
24. Eymard, R. Gallouet, T. R., Herbin, R. The finite volume method. *Handbook of Numerical Analysis*, Vol. VII, 2000, p. 713-1020. Editors: P.G. Ciarlet and J.L. Lions.
25. Baker, J.B.H., J M. Ruohoniemi, K.A. Sterne. SuperDARN ionospheric space weather, *IEEE Aerosp. Electron. Syst. Mag.* 26 (1), 2011, 30-34.
26. Velinov, P.I.Y., L. Mateev. Response of the Middle Atmosphere on Galactic Cosmic Ray Influence. *Geomagnetism and Aeronomy*, 30, 4, 1990, 593-598.
27. Hale, L.C. Middle atmosphere electrical structure, dynamics and coupling, *Adv.Space.Res.*, 4 (4), 1984, 175-186.
28. Mateev, L., P.I.Y. Velinov. 1992, Cosmic Ray Variation Effects on the Parameters of the Global Atmospheric Electric Circuit. *J. Adv. Space Res.*, 12, 10, 353-356.
29. Zadorozhni, B., A. A. Tyutin. Universal diurnal variations of mesospheric electric fields, *Adv.Space Res*, 20, 1997, 2177-2182.